Interaction Analysis of Micro Bubbles in the Flat Plate to Reduce Drag Using Computational Fluid Dynamic

Vicky Adrian Putranto[1], Allessandro Utomo[1], Gunawan[1,*]

[1] Department of Mechanical Engineering, Faculty of Engineering, Universitas Indonesia, Depok City, West Java, 16424 Indonesia

ARTICLE INFO	ABSTRACT
	Ship transportation has become one of the world's main commodities. There are many ways to improve the efficiency of sea transportation, one of them by reducing the resistance on the hull of the ship. The ship drags reduction technique that will be investigated in this experiment is the bubble drag reduction technique. In this simulation, microbubble injection analysis will be carried out to find the flow efficiency on the flat plate in the numerical calculation of ANSYS FLUENT. The equation that will be used in this simulation is Navier Stokes equation and the method that will be used is volume of fluid where the dimensions of the geometry are 90mm x 10mm with the injection bubble located on a flat plate wall with a distance of 30mm from the x-axis. The variations carried out are variations in bubble injection speed of 0m/s, 10.9m/s, 21.8m/s, and 32.7m/s. Then 10 points will be given with a distance of 0.003mm from the plate wall to determine the fluid flow velocity and determine the efficiency of each flow. Efficiency from each simulation is 87.06%, 88.16%, 90.5%, and 84.41%. There is an increase in flow efficiency with the help of micro bubble injection at speeds of 10.9 m/s and 21.8 m/s, respectively, an increase in efficiency of 1.1% and 3.44% which results in the highest efficiency in this simulation. Turbulence resulting from bubble injection starts to appear at a speed of 32.7 m/s thereby reducing the flow velocity and making the efficiency decrease by 2.6%. The flow efficiency increases with the injection of micro bubbles and has the highest value at a speed of 21.8 m/s then the efficiency begins to decrease at a speed of 32.8 m/s due to turbulence.

1. Introduction

Resistance can be thought of as the net force in the direction opposite to the direction of fluid motion [1-3,5-8]. The boundary layer appears when the fluid flows over the surface. A boundary layer as a thin layer in the liquid adjacent to a wall or surface that develops due to viscosity [10,11,14-16,19]. The effect of the boundary layer can be seen in Figure 1 below. In this velocity image, the profile velocity as it approaches the flat plate is uniform, after arriving at the surface the profile velocity changes instantaneously in the area closest to the wall. Inside the boundary layer, the velocity profile of the fluid flows from zero at the wall or solid surface and gradually increases to a constant value, which is the flow velocity outside this region.

* *Corresponding author.*
E-mail address: gunawan_kapal@eng.ui.ac.id

This effect is depicted in Figure 2 where the non-dimensional velocity U/Ue is nearly zero when close to the wall, i.e. for small values of y/δ. As the liquid moves away from the wall and towards the top of the boundary layer, the velocity increases rapidly until it reaches the value of the flow velocity, for example, U/Ue $=y/\delta=1$. The velocity of the fluid on the wall is zero because the non-slip condition of the solid wall causes the fluid particles to stick to the wall. The thickness of the boundary layer increases as the flow moves downstream.
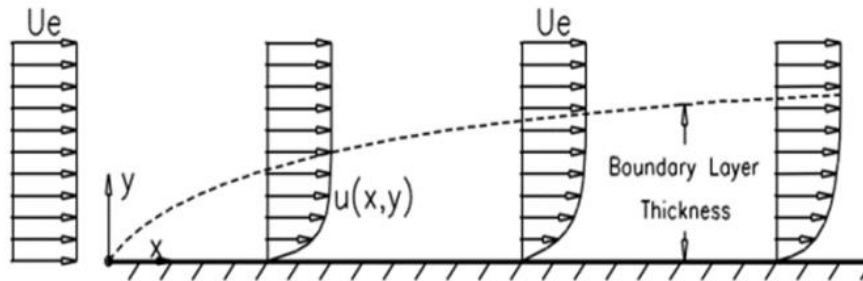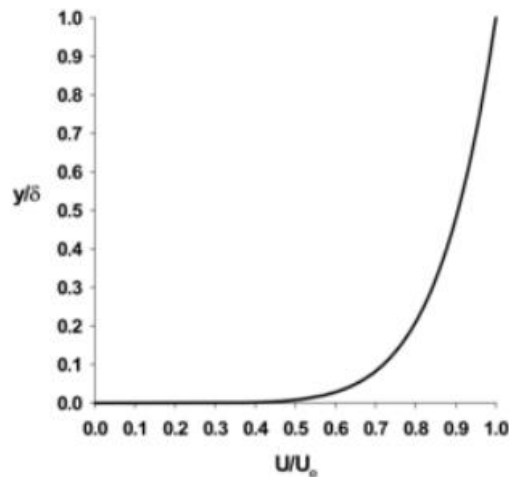

Fig. 1. Boundary layer depiction [4]

Fig. 2. The non-dimensional velocity profile of the boundary layer [4]

There has been previously extensive research on the effects of microbubble gas injection as a drag reduction method. The findings of previous studies are in a positive direction, giving the value of inhibition reduction of up to 80 and 90 percent, respectively. The drag reduction mode occurs because the microbubbles create a lubricating layer within the boundary layer which reduces the interaction between the fluid and the wall. Instead of the liquid particles sticking to the walls, they flow relative to the microbubbles. It is important to note that this method of reducing resistance, although theoretically effective, can depend on several factors such as flow rate, relative density, type of microbubble gas and others. In this simulation, we will see a comparison of the efficiency of various bubble injection speeds.

2. Methodology
2.1 Governing Equations

The study by [9] produced a single-phase computational fluid dynamics model to observe the flow of microbubbles over a flat plate. In the study of [9], water injection and microbubbles were

modelled as a mass source in the first layer of cells on a flat plate. By varying the properties of the gas used for microbubble injection, this study attempted to determine the role of mixture density and density ratio in drag reduction. The coefficient of friction can be defined as friction per unit area divided by the numerator [20]. This coefficient of friction depends on the Reynolds number (Re).

To be effective in determining flow behavior, several systems of equations are used. Due to the turbulent nature of the model, the Reynolds-averaged Navier-Stokes (RANS) equation [9] was used to model the flow. The RANS equation is used because it allows for instantaneous flow properties to be obtained by looking at the combination of the average flow properties and the disturbance values.

$$\frac{\partial \rho}{\partial t} + \frac{\partial}{\partial x_i}(\rho_m u_i) = \dot{m} \tag{1}$$

$$\frac{\partial}{\partial t}(\rho_m u_i) + \frac{\partial}{\partial x_i}(\rho_m u_i u_j) = \frac{\partial p}{\partial x_i} + \frac{\partial}{\partial x_i}\left[\mu_m\left(\frac{\partial u_i}{\partial x_j} + \frac{\partial u_j}{\partial x_i} - \frac{2}{3}\delta_{ij}\frac{\partial u_i}{\partial x_i}\right)\right] + \frac{\partial}{\partial x_i}(-\rho_m u_i' u_j') + \dot{m}u_i \tag{2}$$

In the equation of conservation of momentum, the factor of -⅔ is presented according to the Stokes hypothesis. The use of this equation by the solver can be a potential source of error in calculations. The Stokes hypothesis stating that the coefficient of bulk viscosity is equal to zero was taken as a law for more than a century and is still a topic of controversy in fluid mechanics. While this factor can be thought of as a monatomic gas, it actually has a much larger positive number. There is experimental evidence to show that this factor is almost equal to 1000 for CO_2 [18]. However, the term here is related to the enlarging factor, which can be neglected when the expansion viscosity is very small [17]. In modelling it is used to observe incompressible flow on a wide scale and the ANSYS formulation as well as by [9] can be considered sufficient for this simple model.

In the equation shown, density and viscosity are mixtures. This allows calculations to combine the effects of both species. The density of the mixture is calculated using the volume-weighted mixing law. Based on the recommendations of the ANSYS theoretical guide, the viscosity of the mixture can be calculated using the mass fraction of the average pure species viscosity due to the component-dependent model. This equation is also used by [9] to calculate the viscosity of the mixture and recommend this model. This model seeks to use a simple method that can effectively model the effectiveness of reducing the microbubble barrier and increasing it. There are other methods for viscous mixtures that can yield better results, such as Kirchhoff's law for mixed viscosities.

$$\rho_m = \frac{1}{\Sigma i \frac{Y_i}{\rho i}} \tag{3}$$

$$\mu_m = \Sigma i\, Y i\, \mu_i \tag{4}$$

It is well documented that roughness affects the resistance experienced by fluids in motion. Generally, the roughness acts to limit the movement of the fluid along the wall, causing the fluid particles to adhere further to the wall. This increases the viscous drag and shear stress, decreasing the value of the average velocity profile in the boundary layer. In the solver, the modified wall law for roughness is used to analyse flow behaviour due to wall roughness (ANSYS). The wall law is modified to include the intercept, which depends on the roughness height, +, and the roughness constant, r. This legal treatment uses the definition of the flow regime proposed by [12], where k is

the average roughness height and + indicates the normalization of the roughness height with the unit wall [3]. The relationship is seen by using a system of equations.

$$u^+ = \frac{1}{K}\ln y^+ - \Delta B \qquad (5)$$

The wall coordinates are defined as

$$y^+ = \rho y u_\tau / \mu \qquad (6)$$

The wall function is defined as

$$u^+ = u/u_\tau \qquad (7)$$

The frictional velocity is defined as

$$u_\tau = \sqrt{\tau_w/\rho} \qquad (8)$$

Intercepts are defined using the relationship below

$$\Delta B = \frac{1}{K}\ln f_r \qquad (9)$$

In this case, fr is a roughness function that depends on the roughness condition because currently there is no universal function for all cases.

The governing equations consist of the conservation of mass, Eq. (10), and momentum, Eq. (11).

$$\frac{\partial \rho}{\partial t} + \nabla \cdot (\rho \vec{U}) = 0 \qquad (10)$$

$$\frac{\partial}{\partial t}(\rho \vec{U}) + \nabla \cdot (\rho \vec{U}\vec{U}) = -\nabla P + \nabla \cdot [\mu(\nabla \vec{U} + \nabla \vec{U}^T)] + F_{st} \qquad (11)$$

in which ρ, t, $\vec{U}$, P, and μ donate density, time, velocity vector, pressure, and dynamic viscosity, respectively. Fst is the surface tension force acting at the interface of two immiscible phases. The gravitational acceleration has been neglected since the length scale is in the order of a few microns. In the VOF model, an additional continuity equation is solved to track the interface for the volume fraction of Phase p. αp is a representation of the phase advection.

$$\frac{\partial \alpha_p}{\partial t} + \vec{U}.\nabla \alpha_p = 0 \qquad (12)$$

The portion of each computational cell filled with a specific phase is determined by the volume fraction of that phase using the following ally called an "indicator function", to determine the different phases as well as the position of the interface [13]. This method demonstrates higher

flexibility in handling topological changes and is, therefore, more suitable for microbubble simulation in ideal conditions.

2.2 Computational Fluid Dynamics Setup

Computational Fluid Dynamics (CFD) is a field that, while effective, can have many obstacles that can quickly become a stumbling block for investigators. It is very important to use the correct modelling so that get optimal results. To perform CFD analysis, there are several tools software that are commercially available and can be selected by the researcher. For this research, the ANSYS program is used to model and simulate system behaviour the purpose is simply to compare and test theories and perform analysis. It was chosen because of its strong track record, commercial availability and due to the fact that this software has been used to model the system [9].

The geometry is made with a size of 90 mm x 10 mm with a microbubble inlet on the top wall at a distance of 30 mm from the x-axis. The wall in the section on the geometry measuring 30 mm is the slip wall, then the rest is the non-slip wall. The geometric design can be seen in Figure 3 below.
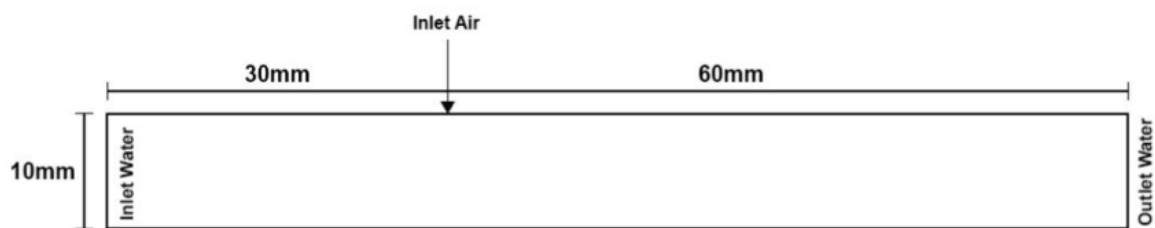

Fig. 3. Geometric design

The meshing made in this experiment uses an element size of 0.0001 so that a meshing of 90010 elements is obtained so that a dense meshing form is obtained so that the data is more convergent. The computational models chosen are:

i. Volume of Fluid
ii. Viscosity – k and ω

The k and ω models are used for modelling turbulence. The values of k and are selected as 1.2×10^{-5} and 1.2×10^{-3} respectively and the values of this are selected for system initialization. The selected ingredients are water (liquid) and carbon dioxide for the mixed model which allows the model to accurately predict the behaviour of the two interacting fluids as a mixture. For the fluid zone, water is selected as the upstream liquid and carbon dioxide gas to act as injected microbubbles.

The cell zone is set to accurately mimic the flow and injection conditions of micro bubbles. There are two differences for cell zones with both zones defined as fluid. The first zone assignment is the microbubble injection area, which is designated as the source term for CO_2 set at a level that matches the values by [9]. The second cell zone which serves as the microbubble injection zone, this area is defined as the fluid zone.

The inlet was defined as an inlet velocity limit condition using values of 10.9 s and 4.2 s which are consistent with the values used by [9]. Symmetry boundary conditions are used at the leading edge of the domain as well as the far-field system which effectively predicts the behaviour of flat plates in waterways. The no-slip boundary condition is applied to all walls which makes the plate act as a flat plate. A constant pressure limit condition is applied at the outlet. System initialization using the inlet as a reference point allows the simulation to adopt the values of k and ω as initial guesses.

3. Results

In the resistance reduction experiment with microbubbles, 4 simulations were carried out with differences in flow velocity at the water inlet, namely 0 M/S, 10.9 M/S, 21.8 M/S, and 32.7 M/S. Variation of the inlet with a speed of 0 M/S will be used as a flow reference in the absence of incoming bubbles. Iterations selected in conducting the simulation amounted to 20 per timestep with a number of timesteps of 500 and the time of each timestep of 0.001s. Total The timesteps performed in one simulation experiment are 10000.

In calculating the fluid flow velocity, 10 points are entered to calculate flow speed. The form of visualization after the inclusion of these 10 points can be seen in Figure 4.
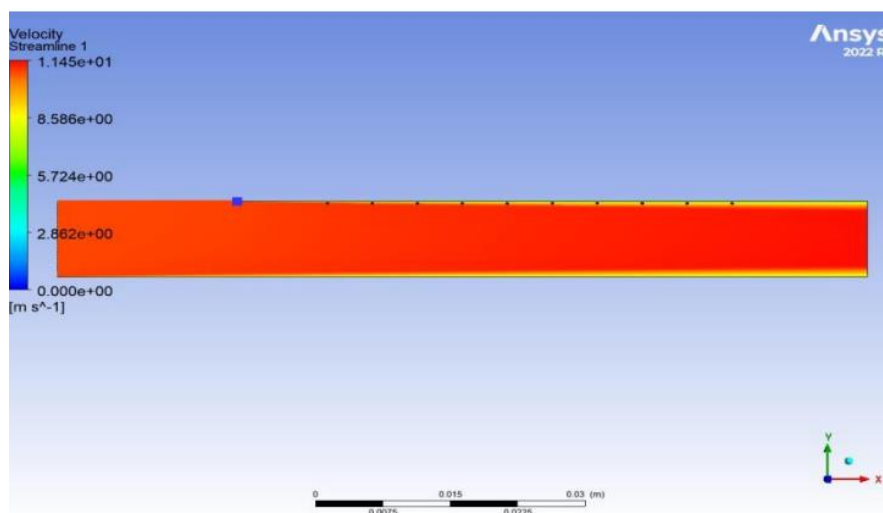

Fig. 4. Injection speed calculation point 0 m/s

The black round dot is the point where the fluid velocity calculation is carried out and the blue box is the injection site for micro bubbles into the system. The results are then exported and the fluid flow velocity can be seen in Table 1 below. The same thing was done at the inlet speed of 10.9 m/s, 21.8 m/s, and 32.7 m/s (Table 2-4).

Table 1
Injection speed 0 m/s at 10 points

No	X	Y	Z	Velocity (m/s)
1	0.03	-0.0003	0.0000506	10.7
2	0.035	-0.0003	0.0000506	10.4
3	0.04	-0.0003	0.0000506	9.97
4	0.045	-0.0003	0.0000506	9.63
5	0.05	-0.0003	0.0000506	9.38
6	0.055	-0.0003	0.0000506	9.20
7	0.06	-0.0003	0.0000506	9.06
8	0.065	-0.0003	0.0000506	8.94
9	0.07	-0.0003	0.0000506	8.85
10	0.075	-0.0003	0.0000506	8.77

Table 2
Injection speed 10.9 m/s at 10 points

No	X	Y	Z	Velocity (m/s)
1	0.03	-0.0003	0.0000506	10.6
2	0.035	-0.0003	0.0000506	10.3
3	0.04	-0.0003	0.0000506	9.93
4	0.045	-0.0003	0.0000506	9.69
5	0.05	-0.0003	0.0000506	9.52
6	0.055	-0.0003	0.0000506	9.39
7	0.06	-0.0003	0.0000506	9.29
8	0.065	-0.0003	0.0000506	9.20
9	0.07	-0.0003	0.0000506	9.12
10	0.075	-0.0003	0.0000506	9.06

Table 3
Injection speed 21.8 m/s at 10 points

No	X	Y	Z	Velocity (m/s)
1	0.03	-0.0003	0.0000506	10.6
2	0.035	-0.0003	0.0000506	10.2
3	0.04	-0.0003	0.0000506	9.96
4	0.045	-0.0003	0.0000506	9.85
5	0.05	-0.0003	0.0000506	9.78
6	0.055	-0.0003	0.0000506	9.73
7	0.06	-0.0003	0.0000506	9.70
8	0.065	-0.0003	0.0000506	9.65
9	0.07	-0.0003	0.0000506	9.61
10	0.075	-0.0003	0.0000506	9.57

Table 4
Injection speed 32.7 m/s at 10 points

No	X	Y	Z	Velocity (m/s)
1	0.03	-0.0003	0.0000506	10
2	0.035	-0.0003	0.0000506	9.34
3	0.04	-0.0003	0.0000506	8.47
4	0.045	-0.0003	0.0000506	6.91
5	0.05	-0.0003	0.0000506	7.14
6	0.055	-0.0003	0.0000506	10.01
7	0.06	-0.0003	0.0000506	10.02
8	0.065	-0.0003	0.0000506	10.03
9	0.07	-0.0003	0.0000506	10.04
10	0.075	-0.0003	0.0000506	10.05

After the fluid flow velocity from the four simulations with variations in air injection speed from 0 M/S, 10.9 M/S, 21.8 M/S, and 32.7 M/S was obtained. Three simulations with speeds of 10.9 M/S, 21.8 M/S, and 32.7 M/S were then compared each with a simulation of 0 M/S to obtain the effect and efficiency of the microbubble injection. In seeking efficiency, the average velocity of the two simulations was calculated and compared with the difference in fluid flow velocity at a distance of 0.0003m from the wall. The calculation of the average speed can be seen in Table 5-7 below.

Table 5
Simulation Comparison of 0 M/S with 10.9 M/S

No	Injection of 0 m/s	Injection of 10.9 m/s
1	10.7	10.6
2	10.4	10.3
3	9.97	9.93
4	9.63	9.69
5	9.38	9.52
6	9.20	9.39
7	9.06	9.29
8	8.94	9.20
9	8.85	9.12
10	8.77	9.06
Mean	9.49	9.61

Table 6
Simulation Comparison of 0 M/S with 21.8 M/S

No	Injection of 0 m/s	Injection of 21.8 m/s
1	10.7	10.6
2	10.4	10.2
3	9.97	9.96
4	9.63	9.85
5	9.38	9.78
6	9.20	9.73
7	9.06	9.70
8	8.94	9.65
9	8.85	9.61
10	8.77	9.57
Mean	9.49	9.865

Table 7
Simulation Comparison of 0 M/S with 32.7 M/S

No	Injection of 0 m/s	Injection of 32.7 m/s
1	10.7	10
2	10.4	9.34
3	9.97	8.47
4	9.63	6.91
5	9.38	7.14
6	9.20	10.01
7	9.06	10.02
8	8.94	10.03
9	8.85	10.04
10	8.77	10.05
Mean	9.49	9.201

From the table above, it can be seen that the average speed of the injection with a velocity of 0 m/s is 9.49 m/s and the average speed of the injection of 10.9 m/s is 9.61 m/s. Due to the flow of water in the system of 10.9 m/s, the resulting increase in efficiency is 1.1%. The average speed of injection with the velocity of 0 m/s is 9.49 m/s and the average speed of injection is 21.8 m/s is 9,865 m/s. Due to the flow of water in the system of 10.9 m/s, the resulting increase in efficiency is 3.44%. Meanwhile, the average speed of injection with a velocity of 0 m/s is 9.49 m/s and the average speed of injection at 32.7 m/s is 9.201 m/s. Because the water flow in the system is 10.9 m/s, the efficiency is reduced by 2.6%.

In the experimental analysis of microbubbles in reducing resistance with variations in injection speed, 4 simulations were carried out. The results can be seen in Figure 5-8 below, where the X axis represents the point and the Y axis represents velocity.
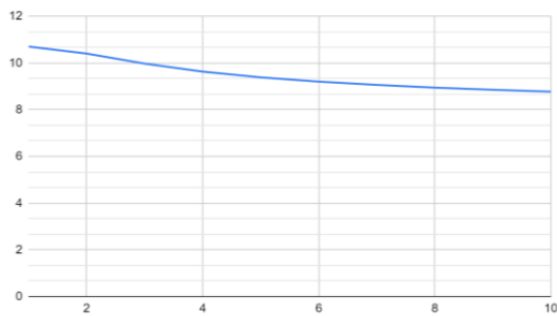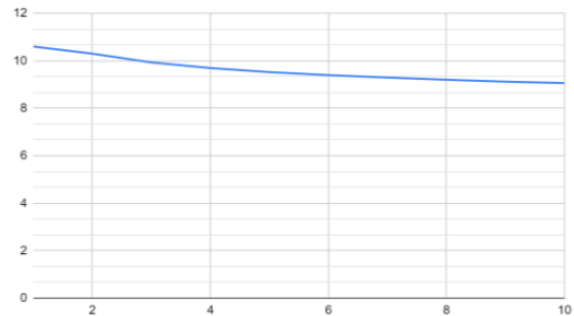

Fig. 5. Velocity of 0m/s

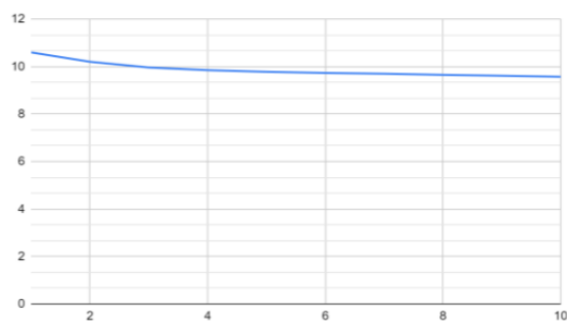**Fig. 6.** Velocity of 10.9m/s

Fig. 7. Velocity of 21.8m/s

Fig. 8. Velocity of 32.7m/s

4. Conclusions

The first simulation uses 0 m/s injection speed to obtain fluid velocity data at a distance of 0.0003 mm from the wall without being influenced by bubble flow with the same fluid flow velocity in all four simulations, namely 10.9 m/s. The velocity of the fluid flowing in this system has an average velocity of 9.49 m/s. Where the flow efficiency is 87.06%.

For the second experiment, a simulation was carried out with the addition of a bubble injection speed of 10.9 m/s. The fluid velocity is then measured at the same distance as the first experiment, which is 0.0003 mm from the wall, then observe the effect of bubbles that appear in the flow. It can be seen from the graph that the injection of micro bubbles into the system can increase the efficiency of fluid flow. The velocity of the fluid flowing in this system has an average velocity of 9.61 m/s. Flow efficiency increased to 88.16%.

The third experiment was simulated with the addition of a bubble injection speed of 21.8 m/s. The fluid velocity is then measured at the same distance as the first experiment, which is 0.0003 mm from the wall, then observe the effect of bubbles that appear in the flow. It can be seen from the graph that the efficiency of the fluid with a velocity of 21.8 m/s has increased compared to the previous experiment. The velocity of the fluid flowing in this system has an average velocity of 9,865 m/s. Flow efficiency increased to 90.5%.

In the fourth experiment, the same simulation as the previous simulation was carried out with the difference in bubble injection speed being 32.7 m/s. For a fixed speed point calculated at 0.0003 m from the wall. As seen in the graph, there is a significant decrease in velocity from point 2 to point 5. This occurs due to the emergence of turbulent flow from the air injection speed which is too large which inhibits the fluid flow rate. It can be seen from the graph of the fourth experiment, that the

flow efficiency actually decreases due to the turbulence, so it can be concluded that the injection flow velocity of 32.7 m/s does not reduce the flow resistance. The average speed of this flow is 9,201 m/s with an efficiency of 84.41%.

There is an increase in flow efficiency with the help of microbubble injection at speeds of 10.9 m/s and 21.8 m/s, respectively, an increase in efficiency of 1.1% and 3.44% which results in the highest efficiency in this simulation. Turbulence resulting from bubble injection starts to appear at a speed of 32.7 m/s thereby reducing the flow velocity and making the efficiency decrease by 2.6%. The flow efficiency increases with the injection of micro bubbles and has the highest value at a speed of 21.8 m/s then the efficiency begins to decrease at a speed of 32.8 m/s due to turbulence.

References

[1] Skudarnov, P. V., and C. X. Lin. "Density ratio and turbulence intensity effects in microbubble drag reduction phenomenon." In *Fluids Engineering Division Summer Meeting*, vol. 41987, pp. 17-22. 2005. https://doi.org/10.1115/FEDSM2005-77075

[2] Cho, Jeremy, Marc Perlin, and Steven L. Ceccio. "Measurement of near-wall stratified bubbly flows using electrical impedance." *Measurement Science and Technology* 16, no. 4 (2005): 1021. https://doi.org/10.1088/0957-0233/16/4/015

[3] Deutsch, Steven, Michael Moeny, Arnold Fontaine, and Howard Petrie. "Microbubble drag reduction in rough walled turbulent boundary layers." In *Fluids Engineering Division Summer Meeting*, vol. 36967, pp. 665-673. 2003. https://doi.org/10.1115/FEDSM2003-45647

[4] Gokcay, S., M. Insel, and A. Y. Odabasi. "Revisiting artificial air cavity concept for high speed craft." *Ocean Engineering* 31, no. 3-4 (2004): 253-267. https://doi.org/10.1016/j.oceaneng.2003.05.002

[5] Utomo, Allessandro Setyo Anggito. "Comparison of Drag Reduction Effect on Barge Model Ship Using Ultrafine Bubble and Microbubble Injection." *Journal of Advanced Research in Fluid Mechanics and Thermal Sciences* 96, no. 2 (2022): 134-143. https://doi.org/10.37934/arfmts.96.2.134143

[6] Utomo, Allessandro Setyo Anggito. "Nano Bubble Lubrication for Flat Plates Skin Friction Reduction." *Journal of Advanced Research in Fluid Mechanics and Thermal Sciences* 81, no. 2 (2021): 14-24. https://doi.org/10.37934/arfmts.81.2.1424

[7] Kawamura, Takafumi, Yasuhiro Moriguchi, Hiroharu Kato, Akira Kakugawa, and Yoshiaki Kodama. "Effect of bubble size on the microbubble drag reduction of a turbulent boundary layer." In *Fluids Engineering Division Summer Meeting*, vol. 36967, pp. 647-654. 2003. https://doi.org/10.1115/FEDSM2003-45645

[8] Kodama, Yoshiaki, Akira Kakugawa, Takahito Takahashi, Satoru Ishikawa, Chiharu Kawakita, Takeshi Kanai, Yasuyuki Toda et al. "A Full-scale Experiment on Microbubbles for Skin Friction Reduction Using" SEIUN MARU" Part 1: The Preparatory Study." *Journal of the Society of Naval Architects of Japan* 2002, no. 192 (2002): 1-13. https://doi.org/10.2534/jjasnaoe1968.2002.1

[9] Skudarnov, P. V., and C. X. Lin. "Drag reduction by gas injection into turbulent boundary layer: Density ratio effect." *International Journal of Heat and Fluid Flow* 27, no. 3 (2006): 436-444. https://doi.org/10.1016/j.ijheatfluidflow.2005.12.002

[10] Madavan, N. K., S. Deutsch, and C. L. Merkle. "Reduction of turbulent skin friction by microbubbles." *The Physics of Fluids* 27, no. 2 (1984): 356-363. https://doi.org/10.1063/1.864620

[11] Merkle, Charles L., and Steven Deutsch. "Microbubble drag reduction in liquid turbulent boundary layers." (1992): 103-127. https://doi.org/10.1115/1.3119751

[12] Nikuradse, Johann. "Stromungsgesetze in rauhen Rohren." *vdi-forschungsheft* 361 (1933): 1.

[13] Day, Philip, Andreas Manz, and Yonghao Zhang, eds. "Microdroplet technology: principles and emerging applications in biology and chemistry." (2012). https://doi.org/10.1007/978-1-4614-3265-4

[14] Pal, S., C. L. Merkle, and S. Deutsch. "Bubble characteristics and trajectories in a microbubble boundary layer." *The Physics of fluids* 31, no. 4 (1988): 744-751. https://doi.org/10.1063/1.866810

[15] Sanders, Wendy C., Eric S. Winkel, David R. Dowling, Marc Perlin, and Steven L. Ceccio. "Bubble friction drag reduction in a high-Reynolds-number flat-plate turbulent boundary layer." *Journal of Fluid Mechanics* 552 (2006): 353-380. https://doi.org/10.1017/S0022112006008688

[16] Sayyaadi, H., and M. Nematollahi. "Determination of optimum injection flow rate to achieve maximum micro bubble drag reduction in ships; an experimental approach." *Scientia iranica* 20, no. 3 (2013): 535-541.

[17] Sonin, Ain A. "Equation of Motion for Viscous Fluids." (2001): 28-30.

[18] Truesdell, C. "The present status of the controversy regarding the bulk viscosity of fluids." *Proceedings of the Royal Society of London. Series A. Mathematical and Physical Sciences* 226, no. 1164 (1954): 59-65. https://doi.org/10.1098/rspa.1954.0237

[19] Utomo, Allessandro, Achmad Riadi, Gunawan, and Yanuar. "Drag reduction using additives in smooth circular pipes based on experimental approach." *Processes* 9, no. 9 (2021): 1596. https://doi.org/10.3390/pr9091596

[20] Von Karman, Th. "Turbulence and skin friction." *Journal of the Aeronautical Sciences* 1, no. 1 (1934): 1-20. https://doi.org/10.2514/8.5